Proceedings of ASME Turbo Expo 2011
GT2011
June 6-10, 2011, Vancouver, British Columbia, Canada

GT2011-46502

TURNING MID TURBINE FRAME BEHAVIOR FOR DIFFERENT HP TURBINE OUTFLOW CONDITIONS

Berardo Paradiso[*], Cornelia Santner, Josef Hubinka, Emil Göttlich

Inst. f. Thermal Turbomachinery and Machine Dynamics
Graz University of Technology, Austria
Email: berardo.paradiso@polimi.it

Martin Hoeger

MTU Aero Engines
Munich, Germany

ABSTRACT

The design of turbine frames with turning vanes, known as turning mid-turbine frames (TMTF), becomes of great importance for high by-pass ratio engines with counter-rotating turbines. To achieve a more efficient low-pressure turbine the overall diffusion and radial offset should be increased. One goal of the EU project DREAM is to analyse the flow through a TMTF and a downstream arranged counter rotating LP rotor. The investigation of these complex interrelationships has been performed in the unique two-spool continuously operating transonic test turbine facility at Graz University of Technology. The test setup consists of an unshrouded HP stage, the TMTF and a shrouded LP rotor. The shafts of both turbines are mechanically independent, so the test rig allows a realistic two shaft turbine operation. The TMTF flow field is highly complex. It is a turbulent and unsteady flow dominated by strong secondary flows and vortex-interactions. The upstream transonic high pressure turbine stage produces a complex inflow with high levels of turbulence, stationary and rotating wakes and vortical structures. Therefore the application of advanced measurement techniques is necessary. To describe the HP-TMTF interaction time-resolved pressure measurements have applied within the project. The TMTF was instrumented with 10 fast response pressure transducers; static pressure tap recordings on the strut and on the TMTF endwalls have been also applied. Five hole probe, total pressure and total temperature rakes have been additionally acquired in the planes just in front of the struts and downstream to evaluate the performance of the TMTF. The results of these conventional techniques are presented in this work and they represent the necessary starting point for the evaluation and the description of the flowfield. The idea is to start the study analysing the mean quantities and the overall performance of the two stages for different conditions and to leave the analysis of the time-resolved results for further investigation. Detailed investigations will start from the data presented in this paper; indeed, the use of unsteady measurement techniques is time consuming and cannot be performed for such a large amount of flow conditions, radial planes and HP vane - TMTF relative positions. Three operating conditions for different clocking positions have been considered. The variation of the operating conditions has been achieved by varying the HP shaft velocity and pressure ratio, with a consequence change of pressure ratio in the LP rotor. For this analysis the LP shaft velocity was kept constant. The TMTF performance variations will be analysed in terms of total pressure loss coefficient and exit flow angle; the mean interaction between the structures coming from the HP stage and the struts will represent the interpretation key to explain these variations. This work is part of the EU project DREAM (ValiDation of Radical Engine Architecture SysteMs, contract No. ACP7-GA-2008-211861).

INTRODUCTION

Since the last decade the biggest aircraft engine companies are interested in reducing fuel consumption, and the political pressure to reduce CO2 has increased considerably. An other important issue is represented by the noise generated in jet engines. Ultra-high-bypass-ratio commercial jet engines characterized by large fan diameters and small high pressure ratio cores is a promising approach to face these problems [1]. These engines require a LP turbine rotating at low velocity but with larger diameter to keep the same load. The connection between the HP and the LP stages is realized by a transition duct (refer to Fig. 2). In order to meet the requirement of low weight, it is desirable to design transition ducts as short as possible, with

[*]Currently affiliated with Dipartimento di Energia, Politecnico di Milano, Milano, Italy

a minimum area ratio (Aout/Ain) of about 0.5 and a large diffusive effect. In several cases a strut is applied in the transition duct which has the function to sustain axial or radial loads; these struts could also allow access for maintenance, like oil pipes. An experimental and numerical work [2] conducted on an engine with a representative high radius ratio inter-turbine diffuser showed that without the struts the flow separates at the casing. Several works were carried out to determine the aerodynamic performance of transition ducts with non-lifting struts [3], [4].

Other authors focused their research on the interaction between the HP stage and the downstream struts in a duct. In two different papers Miller et al described the migration and dissipation of wake, shock and potential field interaction in a transonic high-pressure turbine stage where a swan-necked duct was installed. In the 1^{st} work the authors explained the time-resolved behavior and the three-dimensional migration of the structures generated by the vane/rotor interaction as they convect downstream. The authors also observed that the wake at the inlet plane of the LP vane is extremely weak and the wake has been moved between the mid-height of the passage and the casing wall due to the radial pressure gradient [5]. In his 2^{nd} work Miller et al [6] studied the interaction between a high-pressure rotor and a downstream vane. Measurements were conducted at engine-representative Mach and Reynolds numbers, and data were acquired using a fast response aerodynamic probe upstream and downstream the vane. It was shown that the presence of the upstream stage significantly changes the structure of the secondary flow in the vane and it causes a small drop in its performance. In this last work the influence of the tip leakage flow was studied by a CFD simulation with zero gap size.
At Graz University of Technology the problem was studied in detail by Marn and Göttlich in several works within the EU project AIDA. In [7] and [8] the influence of blade tip gap variation was analysed and time average and time-resolved results were presented. Further the same authors studied the application of an integrated concept (IC) in turbine ducts [9]. In [9] the IC was investigated and compared with a base design. To shorten the intermediate turbine duct length and thus the engine length, the low pressure vane was removed and its function was integrated into the strutted diffuser leading to turning wide chord vanes. The intention of the design was to have a similar duct outflow condition as it has been achieved with the presence of a LP vane. The results showed that a similar flow field can be realised with this IC but that the big secondary structures generated by this large vane have to be taken into account when a LP rotor is placed further downstream. Lavagnoli et al [10] investigated the insertion of splitter vanes between turning struts with the intention to control the growth of big secondary vortices . It has to be remarked that all these tests were never performed with a downstream LP rotor like in engine conditions. This lack of experimental data, also to compare with CFD results, was the reason for adapting the transonic test turbine facility at Graz University of Technology. Within the DREAM project a second shaft was placed and a counter-rotating LP rotor was mounted on it. During the test campaign the relative position between the HP vane and the TMTF was kept constant for what concerns FHP measurements while for rakes and pressure tap readings an analysis of the indexing was carried out.
Indexing, also known as clocking, was widely studied during the last decades by a large number of authors. In LP turbines clocking is directly linked to the wakes [11], while in transonic HP turbines the trailing edge shocks and the secondary flows of the first vane represent a further cause of circumferential non-uniformity for the downstream vane; wakes have little effects compared to other flow structures [12]. The influence of the first vane shock on the rotor aerodynamics has been investigated by a number of authors, Dénos et al. [13] observed significant rotor load fluctuation as a consequence of the shock-rotor interaction; Gadea et al [14] showed, in a 1.5 HP turbine, how the optimum clocking position for aerodynamics did not minimize the unsteady force. However, Haldeman et al [15] observed in a HP turbine a decrease in envelope size of the static pressure for the optimum aerodynamic clocking position. Recently Schennach et al [16] observed that at the first stage exit the rotor hub passage vortex as well as the rotor trailing edge shock are strongly influenced by the first vane shock. Finally the interest in this matter become smaller due to the fact that it was not possible to get, for HP turbines, general conclusions. The results seem to be strongly dependent on the design. Moreover the differences observed are often of the same order of magnitude of the measurement errors. In this work clocking was applied with the aim of analyzing the HP-TMTF design position. The acquisition of additional data in different index positions may provide an additional interpretation key of the complex phenomena occurring on the TMTF surfaces. The transition and possible regions of separation could be influenced by the incoming structures. With clocking it is possible to control the space position where the flow coming from the HP stage impacts the TMTF. In this paper the TMTF pressure distribution is reported for 30 clocking positions and an evaluation of the LP stage performance depending on clocking is also presented.

The present paper shows the first results of measurements obtained on the two spool test rig for three operating conditions and for different vane-strut positions. The authors intention is to analyze the TMTF behavior for a wide range of inlet flow conditions. The objective is to report the overall performance of this component in terms of total pressure loss, secondary flows and load and to study the influence in terms of performance on the downstream LP rotor. The study was intentionally focused on overall quantities to provide a valid basis for further detailed investigations.

EXPERIMENTAL SETUP

Two spool test rig

To allow realistic investigations of the flow through different turning mid turbine frame configurations at the Institute for Thermal Turbomachinery and Machine Dynamics the transonic test turbine facility was modified. An overview of the whole experimental plant is proposed in Fig. 1 The facility is a continuously operating cold-flow open-circuit plant; for the DREAM project a second separated shaft was realized in order to apply a LP rotor. In the first setup the LP rotor is counter-rotating with respect to the HP rotor.

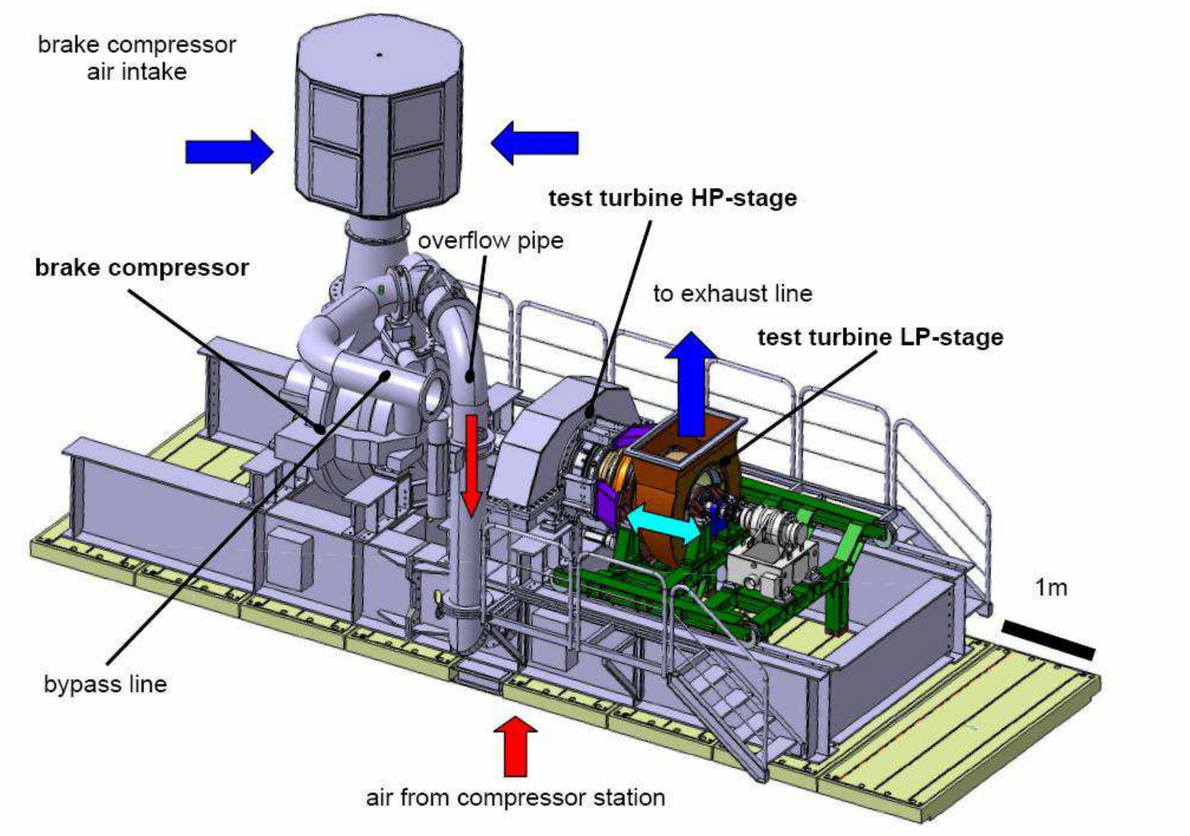

FIGURE 1. TEST RIG OVERVIEW.

TABLE 1. MAIN DESIGN PARAMETERS.

	HP vane	**HP rotor**	**TMTF**	**LP rotor**
vane -blade n	24	36	16	72
pitch/chord ratio	0.89	0.8	n.a.	n.a.
thickness/chord ratio	0.31	0.19	0.22	0.12
aspect ratio H/l_{ax}	1.15	1.37	0.53	2.94
inlet- exit Ma	0.09-1.06	0.47-0.95	n.a.	n.a.
$Re_C * 10^{+6}$	2.38	1.1	1.86	0.46
$\Delta\alpha(\Delta\beta)[deg]$	71	106.7 (72.7)	n.a.	n.a
work parameter $\Delta h/u^2$	-	1.624	-	n.a.
flow parameter c_{ax}/u	-	0.531	-	n.a.
degree of reaction r	-	0.338	-	n.a.

This unique configuration allows to test rig inserts with a diameter up to 800 mm under engine-representative conditions. To ease the investigations of test setups with different axial lengths both turbines are designed with overhung-type turbine shafts. Together with the LP turbine, mounted on a frame which is movable in axial direction, it allows easy disk assembly without dismantling the bearings and the simple application of transition duct and TMTF designs with different axial lengths. The facility is driven by pressurized air delivered by a separate 3 MW compressor station in the second basement of the institute. The shaft power of the HP stage drives a three-stage radial brake compressor. This brake compressor delivers additional air mixed to the flow from the compressor station and increases the overall mass flow. The air temperature at turbine stage inlet can be adjusted by coolers from 313 K to 450 K . The maximum shaft speed of the HP stage is limited

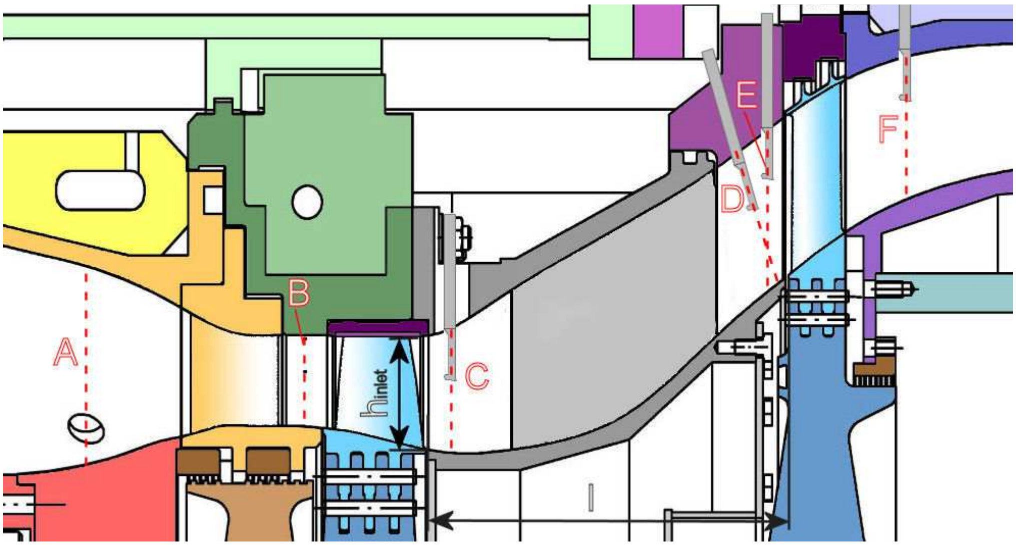

FIGURE 2. TEST SECTION OVERVIEW TOGETHER WITH MEASUREMENT POSITIONS.

to 11550 rpm. Depending on the stage characteristic a maximum coupling power of 2.8 MW at a total mass flow of 22 kg/s can be reached. The power of the LP turbine is absorbed by a water brake with a maximum brake power of 700 kW. Detailed information on the design and construction of the original one stage facility can be found in [17] and [18]. For the design of the LP-stage together with the TMTF see Hubinka et al [19].

Test Setup

The investigated test setup consists of a single stage transonic HP turbine with choked vanes, an s-shaped turning mid turbine frame followed by a shrouded counter-rotating LP turbine. Fig. 1 represents a meridional section of the test facility with the TMTF design. The design of this test configuration was developed by MTU Aero Engines with the aim of investigating the flow in a TMTF that replace the vanes of a LP turbine stage. The rig operated under engine like inlet conditions i.e. strong turbulence structures generated by the complex shock system of the transonic HP turbine, three dimensional boundary layer on the TMTF surfaces and endwalls. Little is known about transition under these conditions, due to the big diameter of the leading edge the TMTF chord length, the prediction of the evolution of secondary structures and vortical flow becomes critically important. Table 1 displays the main design parameters for the two stages. The HP turbine consists of 24 vanes and 36 blades, the stator is choked and it produces a strong shock at the exit. For the LP stage a blade count of 16 struts and 72 blades was chosen in order to minimize the risk of excitation of the LP turbine blades. The resulting machine periodicity is 90 deg, the periodicity is two TMTF (45 deg). This blade count leads to a reduced computational cost while performing unsteady CFD calculations. The incoming air is accelerated by the HP vanes in circumferential direction and it impinges on the HP rotor designed with a cylindrical outer contour. The flow is turned by the TMTF struts in negative direction relative to the rotation of the HP rotor and then the air enters the counter-rotating LP turbine at a larger diameter. Further downstream the flow leaves the test setup through the straight profiled support struts of the front bearing shield and the downstream diffuser. The diffuser and the exhaust casing ware designed in order to maximize the pressure recovery.

Measurement Setup

The rig is instrumented with rakes of Kiel probes to measure the total magnitude of pressure and temperature in three axial planes (A, C and F). The Kiel probe head geometry was chosen because it is not sensitive to changes in yaw and pitch angle in the range of ± 30 deg, and it is therefore useful when the probe alignment with the flow direction is variable. These values are basically read to adjust the operating condition. Due to the rig design rakes could be easily traversed and used to perform easy performance measurements. The HP vanes as well as the outer casing downstream the TMTF are fully rotatable in circumferential direction over 360 deg.

The full description of the time mean flowfield is provided by a FHP placed in planes C, D, F and E. The probe was traversed over one HP stator pitch in plane C and over two strut pitches downstream of the TMTF to gain the full periodicity between the two rows. Radial traverse was realized by a linear stage driven by a stepping motor. Due to the strong inclination of the duct downstream the turning struts a probe with an inclined head of 25 deg relative to the machine axis was applied.

TABLE 2. MEASUREMENT UNCERTAINTIES FOR THE FHP MEASUREMENTS.

Mach	[-]	0.005	-0.004
Yaw	[deg]	0.3	-0.3
Pitch	[deg]	0.5	-0.4
pt	[mbar]	3	-3
p	[mbar]	5.4	-5.1
Tt	[deg]	0.6	-0.5
T	[deg]	0.7	-0.8

TABLE 3. OPERATING CONDITIONS.

		Aero des. point		Off des. point I		Off des. point II	
		HP	LP	HP	LP	HP	LP
pressure ratio	-	3	1.3	2.21	1.2	2.6	1.1
pressure ratio [%des]	-	100	100	75	92	88	85
reduced speed (Nr)	$[rpm/\sqrt{K}]$	525	193	420	189	487	193
reduced mass flow (Qr)	$[kg\cdot\sqrt{K}/s\cdot bar]$	81	218	81	165	81	187

Additional information is provided by pressure readings on the strut pressure side, suction side and the endwalls of the TMTF.

The acquisition system includes 15 multi channel pressure transducers PSI 9016 (240 channels, accuracy of 0.05 % full scale) and four National Instruments Field Point FP-TC-120 input modules (40 channel J thermocouple, accuracy 0.35 deg). Table 2 shows the measurement uncertainties of the quantities directly measured by the FHP. These values contain the error due to the approximation of the probe and due to the systematic error of the PSI Modules and of the Field Point system. The measurement uncertainties of the static pressure taps are ±1 mbar.

Operating Conditions

Three different operating conditions have been tested. For the design (des) condition the HP stage presents a pressure ratio of 3 and the LP turbine has a pressure ratio of 1.3. The Mach number at the TMTF inlet is about 0.5 and it is representative for realistic duct inlet conditions of modern jet engines with a single stage HP turbine at cruise operating conditions. The two additional operation conditions were applied to provide different flow angles for the TMTF. Table 3 reports detailed information of the three tested points in terms of pressure ratio, reduced speed and reduced mass flow. The three conditions were kept while the HP stator-strut indexing is modified for 30 equi-spaced positions.

RESULT AND DISCUSSION

In the following paragraphs the results are presented for the three operating conditions. The flow leaving the HP stage is analysed using the results obtained by FHP, an evaluation of the stage performance is proposed afterwards. Together with the yaw angle and the Mach number the following quantities are presented:

$$Cp = \frac{p-\overline{p_C}}{\overline{pt_C}-\overline{p_C}} \quad (1)$$

$$Cpt = \frac{pt-\overline{p_C}}{\overline{pt_C}-\overline{p_C}} \quad (2)$$

$$\eta = \frac{\overline{Tt_A}-Tt_C}{\overline{Tt_A}-Tt_{C,is}} \quad (3)$$

The next section is devoted to a description of the flow in the duct section with the introduction of a loss coefficient measured across the TMTF. This quantity shows a strong dependence of the TMTF loss mechanisms on the inlet conditions. The consequence on the efficiency of the LP stages is also reported. The influence of indexing is finally discussed for the presented operating points.

HP rotor exit

The pitchwise mass average value of the yaw angle along the span (Fig 3) shows the same structures for the three cases. The tip region dominated by the tip leakage results into an axial flow direction; also the total pressure coefficient increases for the same reason. The lower region between the tip and midspan shows the biggest differences. This phenomena is observed because different pressure ratios across the first nozzle generate unequal secondary structures and then, afterwards, this flowfield encounters a rotor running with a different speed. A high speed region, placed just above midspan, is associated with a pronounced underturning. The increase of the flow angle leads to a reduction in the work exchange and, hence, high total pressure and temperature are observed in the same area. The effect of underturning is linked with the rotor speed and hence more detrimental effects are found for 80%NrHP (off-design condition I) than for 92.7%NrHP (off-design condition II). The efficiency plot confirms the reduction of work exchange; the overall efficiency reveals a reduction of about 4% for 80%NrHP and 0.5% for 92.7%NrHP.

Moving towards the hub, the change of angle reveals traces of secondary structures coming from the HP vanes and spread along the pitch by the rotor. The centre of this vortex is placed where the lowest Mach number is encountered. The first bend of the duct increases the positive pressure gradient from tip to hub.

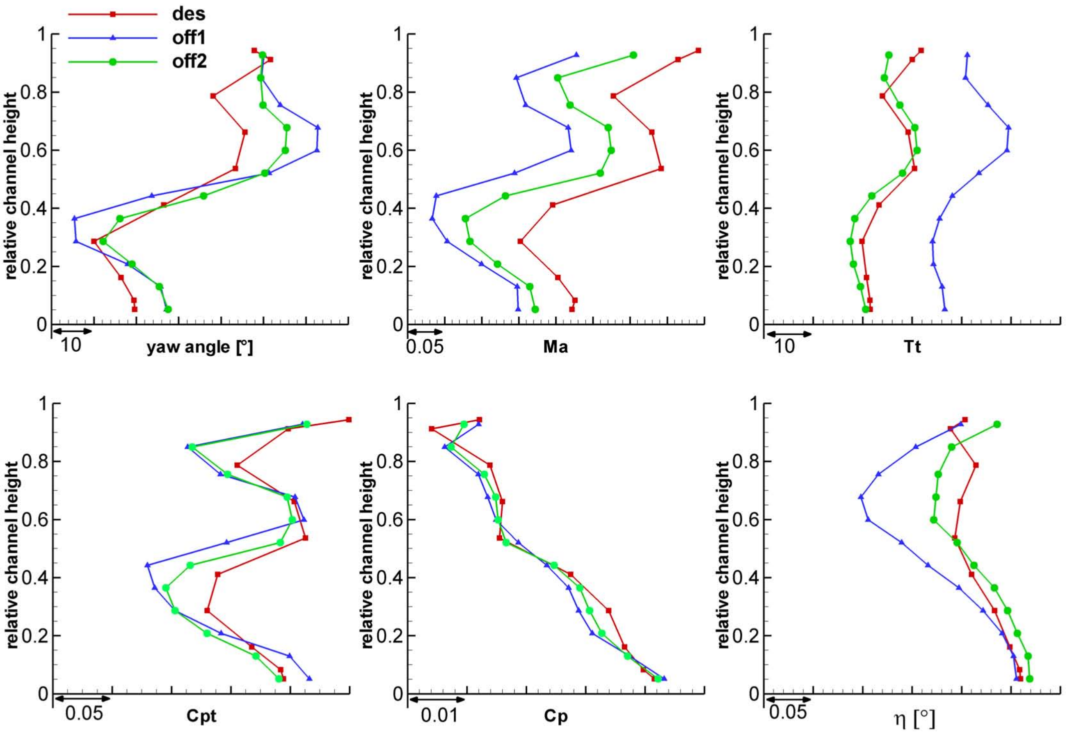

FIGURE 3. MASS AVERAGED RESULTS HP ROTOR EXIT (PLANE C).

TMTF static pressure distribution

In this paragraph the distribution of the pressure coefficient Cp on the pressure and suction side of the TMTF is presented for the three operating points. It is measured along three lines, placed respectively at 25%, 50% and at 75% of the blade height. Based on Fig. 4 - 6 some general considerations about the TMTF design can be done. The peak suction on the SS occurs at about 75% of the strut axial chord. This is the result of the aft loaded design commonly used with the intent to reduce the growth of large secondary vortices. For the design condition the stagnation point is shifted along the whole span on the SS of the TMTF as result of a negative incidence angle. Afterwards the flow is accelerated along the SS up to 75%. At 25% span the incidence appears even more negative while at 75% the flow approaches the nose of the strut with small incidence and for 80%NrHP the incidence turn into positive direction.

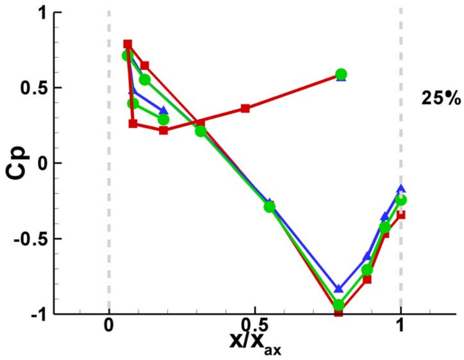

FIGURE 5. STATIC PRESSURE DISTRIBUTION ALONG THE TURNING STRUT AT 25% SPAN.

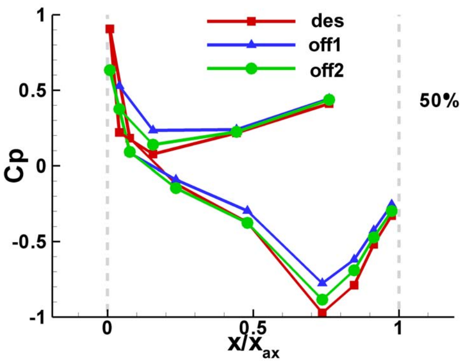

FIGURE 4. STATIC PRESSURE DISTRIBUTION ALONG THE TURNING STRUT AT 50% SPAN.

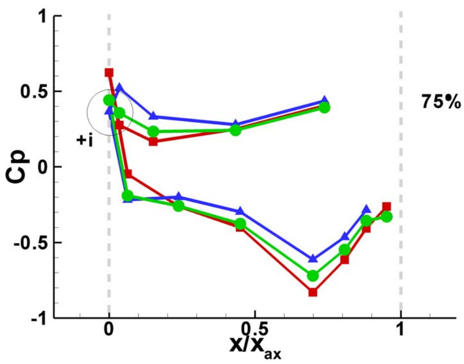

FIGURE 6. STATIC PRESSURE DISTRIBUTION ALONG THE TURNING STRUT AT 75% SPAN.

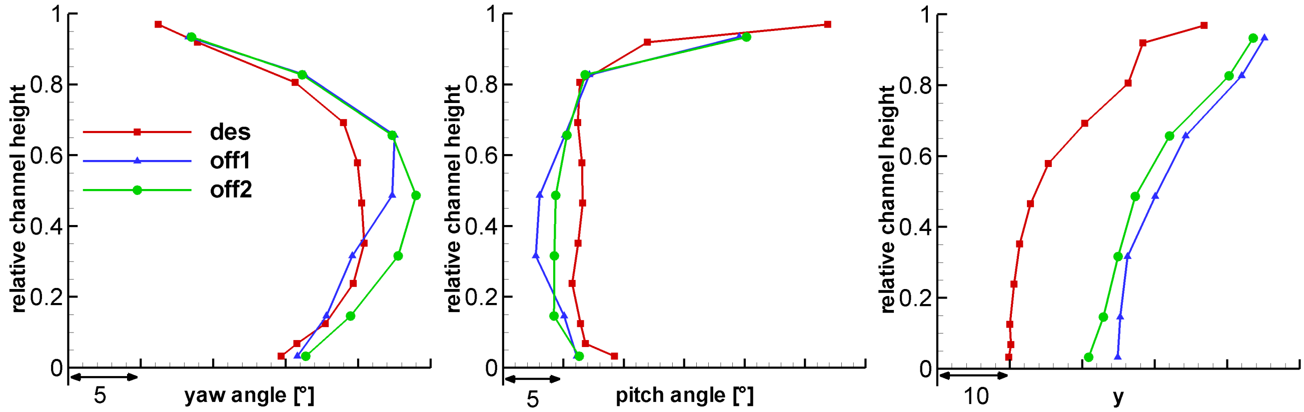

FIGURE 7. MASS AVERAGED RESULTS TMTF EXIT (PLANE D).

The evolution on the PS is gradual and does not present any steep gradients, the results show that the TMTF is more loaded close to the hub where the risk of separation is higher. A CFD calculation performed at MTU showed a corner separation at 5% span in the rear part of the strut SS; however this experimental data hasn't captured this feature. The comparison between the three operating points shows a displacement of the blade load towards the leading edge, this effect appears more pronounced for 80%NrHP. Larger secondary vortices are expected at the TMTF exit for the two off-design conditions compared with the aero-design condition.

TMTF exit flow field

The flow leaving the TMTF before entering the LP rotor is measured in plane D. The endwalls in this position present a pronounced inclination with respect to the machine axis. Measurements with FHP were carried out in a plane inclined respect to the turbine shaft to keep the probe within its calibration range (see Fig.2). Measurements were repeated along two complete pitches (45 degrees) for the design condition and over one strut pitch for the two off design points. In order to evaluate the performance of the TMTF, in addition to the LP stage efficiency, a total pressure loss coefficient is proposed. The total pressure measured in plane D is compared with a reference pressure acquired in plane C as follows:

$$y = \frac{\overline{pt_C} - pt_D}{\overline{pt_C} - p_D} \tag{4}$$

this quantity is pitchwise mass averaged and is presented in Fig. 7 together with the yaw and pitch angle along the span. The design condition shows a more homogeneous trend along the span than the two off-design conditions. The maximum angle variation measured along the blade height for both yaw and pitch is of 5 less for aero-design. The flow results uniform at the LP rotor inlet. The tip area is dominated by strong radial gradients traces of secondary vortices activities. The region between 20 and 70% span reveals the big difference between the three conditions. The right graph of Fig.7 depicts the aforementioned loss coefficient over the span. The condition that displays the worst behavior is 80%NrHP with a decrement of the performance with respect to the design condition of 24%; the difference between 92.7%NrHP and 80%NrHP is within 2%. This reveals that these two working points far from the cruise condition lead to a prominent reduction of the TMFT aerodynamic performances. Nevertheless the flow approaching the LP rotor appears uniform along the span. It means that for each condition the TMTF was able to replace the LP stator. This is paid in terms of total pressure losses but an overall estimation of the second stage performance is essential to establish the real behavior of the TMTF in the off-design conditions. To comprehend the generation of these important differences the analysis of the secondary structures in plane D is required; it is the author's opinion that the generation of such remarkable losses is linked with the different size of the vortices generated in the duct channels and their evolution inside the TMTF. In Fig. 8, Fig. 9 and Fig. 10 the yaw angle distribution (left side) together with the total pressure coefficient (right side) is depicted. By using the yaw angle distribution together with the pitch angle an estimation of the main vortical features is proposed. The Cpt minima traces the position of the loss cores. The zone placed at 25% pitch and spread across the whole span is the trace of the TMTF wake that became stronger after merging with the structures leaving the blade close to the endwalls. An example of that is clearly visible in the upper side of the wake where a counter-clockwise vortical structure is centered in a loss core; this vortex could be recognized as a trace of the Tip Passage Vortex (TPV). A second relevant vortical structure that covers the lower side of the span could be instead identified as the Hub Passage Vortex (HPV).The HPV generated in the TMTF is enforced by the remains of the HP rotor tip leakage vortex and lower passage vortex. These two rotor structures mix out on their way through the TMTF but their vorticity diffuses across the passage and result in this rotating feature. Additional differences were observed in the freejet area where Cpt shows a maximum in correspondence to the HPV core for the off design conditions. This means that the HPV generated in the TMTF is larger than the one leaving the struts for the aero-design point; this is also in accordance with what was observed in the static pressure distribution on the TMTF. The highest magnitude of the HPV is encountered for off1 where also a displacement of the loading towards the leading edge was observed.

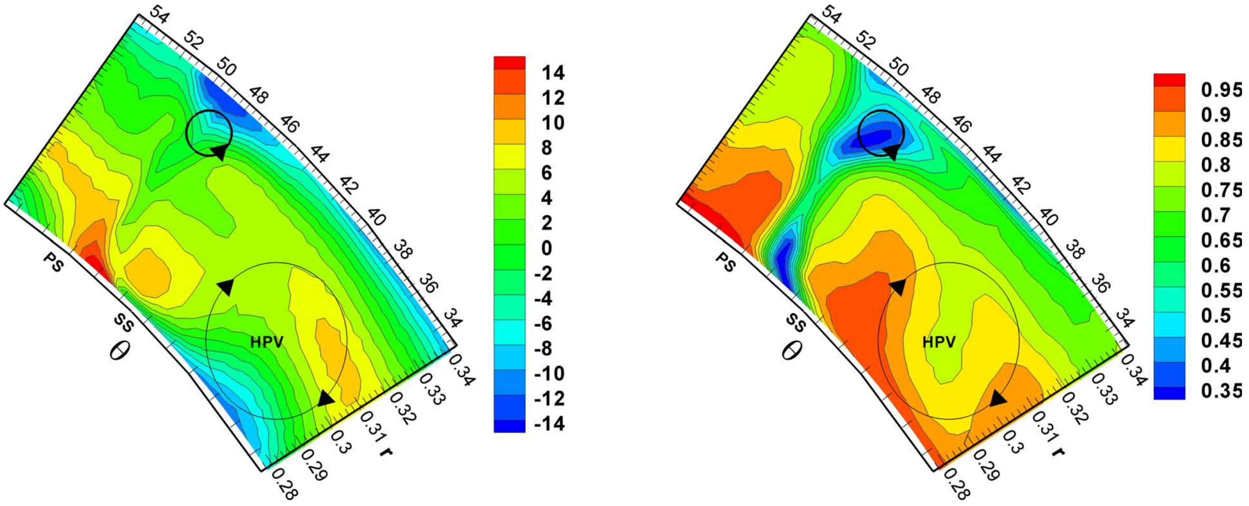

FIGURE 8. YAW ANGLE DISTRIBUTION (LEFT) AND Cpt (RIGHT) TMTF EXIT (PLANE D) FOR DESIGN CONDITION.

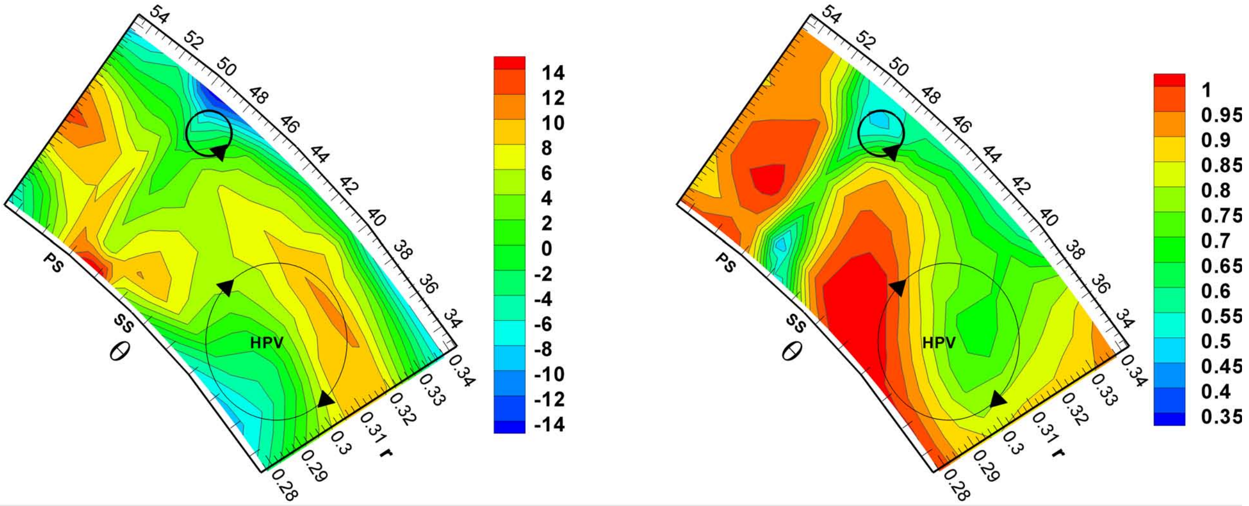

FIGURE 9. YAW ANGLE DISTRIBUTION (LEFT) AND Cpt (RIGHT) TMTF EXIT (PLANE D) FOR 80%NrHP.

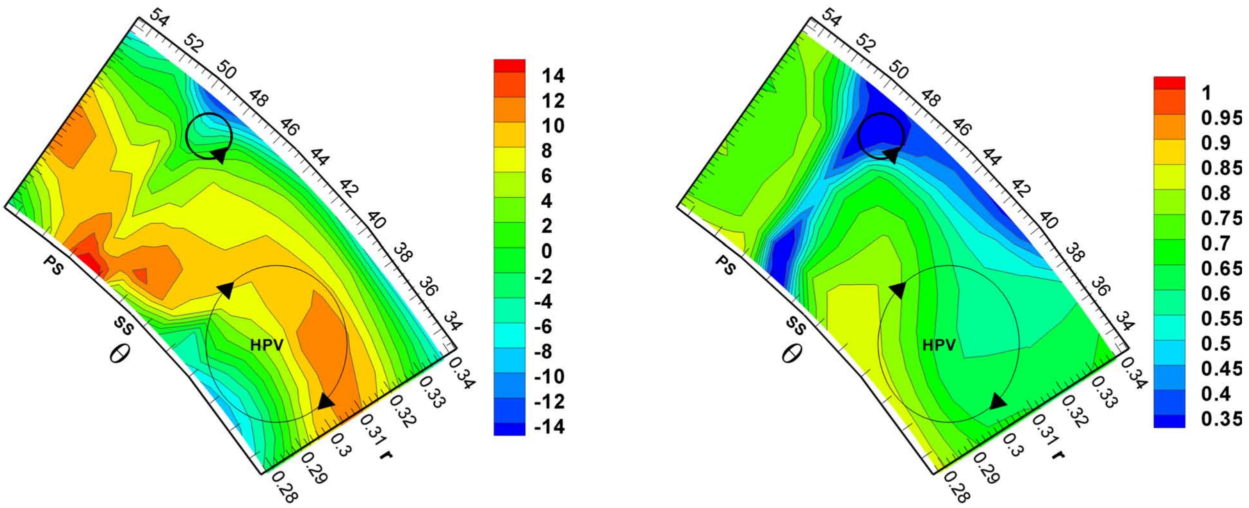

FIGURE 10. YAW ANGLE DISTRIBUTION (LEFT) AND Cpt (RIGHT) TMTF EXIT (PLANE D) FOR 92.7%NrHP.

LP stage performance

In order to establish the effects of the changing incidence angle on the overall performance of the second stage the authors propose an analysis of the results acquired by the rakes. Reference values of pressure and temperature were chosen for the three operating conditions in plane C. The rakes were traversed in plane F for one strut pitch. The results, not presented in detail, showed an increase of the performance for 80%NrHP and 92.7%NrHP with respect to the design contition of 4-5 %. This is not a surprise because as mentioned before the analysis of the TMTF could not end just with a quantification of the pressure losses. It was observed how for the three configurations the struts could guide the flow presenting a very uniform mean flow at the rotor inlet. It is important to consider that the LP rotor is not changing its velocity in the three proposed operating points and for similar inflow conditions presents the same outflow flowfield. Instead, small variations on the inlet conditions could make the LP rotor work in better conditions. This interesting observation will be taken under consideration in future analysis also with the help of unsteady pressure measurements performed downstream the rotor.

Clocking analysis

Before starting the analysis of the different clocking positions a detailed description of the flow at the HP stage exit is necessary. Any spatial non-uniformity represents a potential for clocking. The HP vane-rotor interaction produces a flow at the rotor exit where the periodicity of the upstream vane is still visible especially when the nozzle produces strong shocks (Paradiso at al. [20]). In Fig. 11 and in Fig. 12 the yaw angle distribution and the total temperature contours are depicted. To help the discussion regions of high value of Cpt are marked with dark-grey lines. If the rotor flow field were steady in the relative frame a tangentially uniform flow angle would arise from the time-average of the rotor secondary flows. The presence of stator-rotor interaction produces a periodic modulation of the rotor secondary vortices. Two distinct regions of interaction could be observed; the first, placed between the hub and

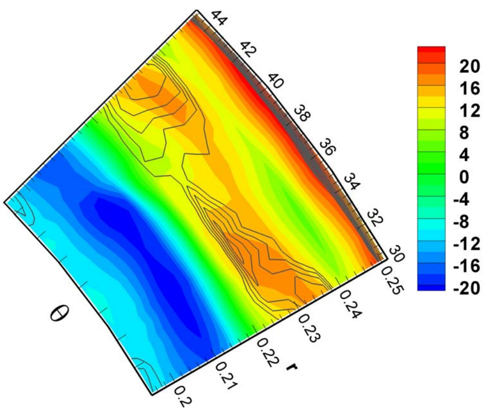

FIGURE 11. YAW ANGLE DISTRIBUTION HP ROTOR EXIT (PLANE C) FOR DESIGN CONDITION.

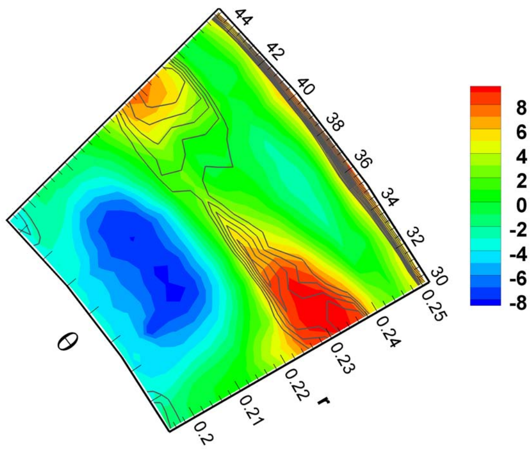

FIGURE 12. TOTAL TEMPERATURE DISTRIBUTION HP ROTOR EXIT (PLANE C) FOR DESIGN CONDITION.

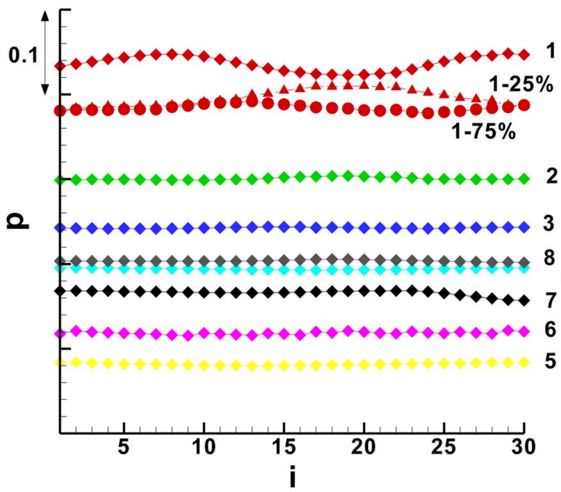

FIGURE 13. TMTF SS PRESSURE DISTRIBUTION vs CLOCKING POSITION.

midpan and a second in the upper part of the channel. The angle distribution and the presence of low Cpt and low Tt suggested that a big exchange of work occurred in this area due to an overturning of the flow. On the other hand the second interaction region reveals a reduced exchange of work linked with underturning. The midspan region appears rather uniform and it is not expected to induce clocking effects. The tip is dominated by the tip leakage flow with an energized flow that has not exchanged its energy with the rotor. In Fig.13 the pressure levels on the SS of the TMTF vs. the clocking position are presented. The data is presented for the design condition, similar consideration could be done for the two off-design conditions. In the graph the position of the pressure tap along the chord is marked: number one corresponds to the pressure on the TMTF nose. Just for this position the behavior for three blade height is also presented. The larger variation of pressure depending on the clocking position is observed on the leading edge of the strut. The biggest change is encountered for the first half of the TMTF while at 75% little fluctuation is found. The changes on

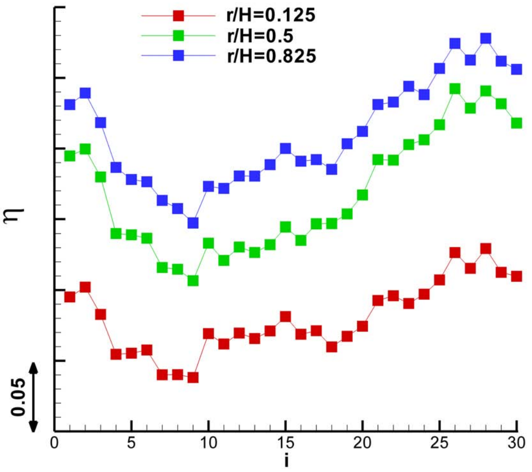

FIGURE 14. LP EFFICIENCY vs CLOCKING POSITIONS.

the PS are not comparable since the results are 20% of what was observed on the SS. This finding underlines how clocking effects are visible on the struts therefore a future analysis that will use high response pressure transducers and hot film technique is planned. The study of the TMTF boundary layer development must take into account also clocking effects especially on the SS surface.

The possible effects of clocking on the LP stage efficiency are analysed using the η coefficient previously described. Again three different channel height position are considered. The rakes recordings were used to calculate the efficiency at the LP rotor exit. In Fig. 14 the results are depicted. The performance changes are small in magnitude and appear larger in the midspan-tip region. It is difficult to link these observation with the changes of pressure level on the TMTF SS because what occurs in the duct channel has to be studied in more detail. These observations need to be discussed when additional data will be provided.

NOMENCLATURE

$TMTF$	Turning mid turbine frame
HP	High pressure
LP	Low pressure
PS	Pressure side
SS	Suction side
yaw	Blade to blade absolute flow angle
$pitch$	Radial flow angle
p	Pressure
pt	Total pressure
T	Temperature
Tt	Total temperature
Cp	Static pressure coefficient
Cpt	Total pressure coefficient
y	Total pressure loss coefficient
η	Stage efficiency (total/total)
HPV	Hub passage vortex
Superscripts	
$-$	Pitchwise mass average

CONCLUSION

The first part of a wide research program was concluded and the results of the time mean results are presented in this paper. The unique test rig realized at Graz University of Technology allows the study of modern jet-engine intermediate turbine ducts in realistic two spool conditions. The use of conventional pressure and temperature measurements techniques together with the test rig capability of performing full traversing allow the measurement of different flow conditions in several measurement planes. Three operating conditions for different HP vanes - struts positions have been considered. A study of the HP stage aerodynamic performance was proposed and a quantitative comparison among the different operating conditions was carried out. The flow in the TMTF was then observed. The evaluation of the loading along the span was object of discussion. For the base design an aft-loaded condition coupled with a negative incidence on the strut nose was observed. The change of HP rotational speed mainly modifies the position of the stagnation point and consequently the load is moved upstream. The off design conditions present a major load in the front part of TMTF. The same conditions show a different secondary flow pattern at TMTF outlet, which means a growing of the hub passage vortex inside the channel. Indeed the meanflow quantities remain more uniform and result in a similar LP rotor performance. The overall performance measured over the LP stage reports small differences for the three points and the best performance was found for 92.7%NrHP. A clocking analysis based on conventional measurements was also proposed. The results are interesting and they encourage the authors in a further analysis.

ACKNOWLEDGMENT

This work was supported by the European Union within the EU-project DREAM (ValiDation of Radical Engine Architecture SysteMs, contract No. ACP7-GA-2008-211861) and the Austrian Ministry for Education, Science and Culture (BMBWK). The authors would like to thank the colleagues of MTU Aero engine that have made possible to realize this work and give the possibility to share and publish these results. The support of Dr. H. P. Pirker in the operation of the compressor station are gratefully acknowledged

REFERENCES

[1] Lord, W. K., MacMartin, D. G., and Tillman, T. G., 2000. “Flow control opportunities in gas turbine engines”. In AIAA Fluids 2000 Conference, Denver, CO, AIAA Paper 2000-2234,2000.

[2] Norris, G., Dominy, R. G., and Smith, A. D., 1998. “Strut influences within a diffusing annular s-shaped duct”. In ASME Paper 98-GT-425.

[3] Wallin, F., Osso, C. A., and Johansson, G., 2008. “Experimental and numerical investigation of an agressive intermediate turbine duct: Part 1 - flowfield at design inlet conditions”. In 26 th AIAA Aplied Aerodynamics conference, AIAA-2008-7056.

[4] Osso, C. A., Wallin, F., and Johansson, G., 2008. “Experimental and numerical investigation of an agressive inter-

mediate turbine duct: Part 2 - flowfield under off-design inlet conditions". In 26 th AIAA Aplied Aerodynamics conference, AIAA-2008-7055.

[5] Miller, R. J., Moss, R. W., Ainsworth, R. W., and Harvey, N. W., 2003. "The development of turbine exit flow in a swan-necked inter-stage diffuser". In Proceedings of ASME Turbo Expo 2003, June 16-19, Atlanta, Georgia, USA, ASME Paper GT-2003-38174.

[6] Miller, R. J., Moss, R. W., Ainsworth, R. W., and Harvey, N. W., 2004. "The effect of an upstream turbine on a low-aspect ratio vane". In Proceedings of ASME Turbo Expo 2004, June 14-17, Vienna, Austria, ASME Paper GT-2004-54017.

[7] Marn, A., Göttlich, E., Pecnick, R., Malzacher, F. J., Schennach, O., and Pirker, H. P., 2007. "The influence of blade tip gap variation on the flow through an agressive s-shaped intermediate turbine duct downstream a transonic turbine stage - part 1: Time-averaged results". In Proceedings of ASME Turbo Expo 2007, May 14–17, Montreal, Canada, ASME Paper GT-2007-27405.

[8] Göttlich, E., Marn, A., Pecnick, R., Malzacher, F. J., Schennach, O., and Pirker, H. P., 2007. "The influence of blade tip gap variation on the flow through an agressive s-shaped intermediate turbine duct downstream a transonic turbine stage - part 2: Time-resolved results and surface flow". In Proceedings of ASME Turbo Expo 2007, May 14–17, Montreal, Canada, ASME Paper GT-2007-28069.

[9] Marn, A., Göttlich, E., Cadrecha, D., and Pirker, H. P., 2009. "Shorten the intermediate turbine duct lenght by applying an integrated concept". *ASME Journal of Turbomachinery,* ***131***.

[10] Lavagnoli, S., Yasa, T., Paniagua, G., Duni, S., and Castillon, L., 2010. "The influence of blade tip gap variation on the flow through an agressive s-shaped intermediate turbine duct downstream a transonic turbine stage - part 1: Time-averaged results". In Proceedings of ASME Turbo Expo 2010, June 14-18, Glasgow, Scotland, UK, ASME Paper GT-2010-22547.

[11] Huber, F. W., Johnson, P. D., Sharma, O. P., Staubach, J. B., and Gaddis, S. W., 1996. "Performance improvement through indexing of turbine airfoils: Part 1-experimental investigation". *ASME Journal of Turbomachinery,* ***118***(4), pp. 630–635.

[12] Miller, R. J., Moss, R. W., Ainsworth, R. W., and Horwood, C. K., 2003. "Time-resolved vane-rotor interaction in a high-pressure turbine stage". *ASME Journal of Turbomachinery,* ***125***(1), pp. 1–13.

[13] Dénos, R., Arts, T., Paniagua, G., Michelassi, V., and Martelli, F., 2001. "Investigation of unsteady rotor aerodynamics in a transonic turbine stage". *ASME Journal of Turbomachinery*.

[14] Gadea, J., Dénos, R., Paniagua, G., Billiard, N., and Sieverding, C. H., 2004. "Effect of clocking on the second stator pressure field of one and a half stage transonic turbine". *Proceedings of ASME Turbo Expo 2004, June 14-17, Vienna, Austria, ASME Paper GT2004-53463*.

[15] Haldeman, C. W., Dunn, M. G., Barter, J. W., Green, B. R., and Bergholz, R. F., 2005. "Experimental investigation of vane clocking in a one and one-half stage high pressure turbine". *ASME Journal of Turbomachinery,* ***127***(3), pp. 512–521.

[16] Schennach, J., Woisetschläger, J., Paradiso, B., Persico, G., and Gaetani, P., 2010. "Three dimensional clocking effects in a one and a half stage transonic turbine". *ASME Journal of Turbomachinery,* ***132***(1).

[17] Erhard, J., and Gehrer, A., 2000. "Design and construction of a transonic test turbine facility". In Proceedings of ASME Turbo Expo 2000, May 8-11, Munich, Germany, ASME paper GT2000-480.

[18] Neumayer, F., Kulhanek, G., Pirker, H. P., Jericha, H., Seyr, A., and Sanz, W., 2001. "Operational behavior of a complex transonic test turbine facility". In Proceedings of ASME Turbo Expo 2001, June 4-7, New Orleans, Louisiana, US, ASME paper GT2001-489.

[19] Hubinka, J., Santner, C., Paradiso, B., Malzacher, F., Göttlich, E., and Heitmeier, F., 2009. "Design and contruction of a two shaft test turbine for investigation of mid turbine frame flows". In Proceedings of ISABE 2009, Sep 7 - 11, Montreal, Canada, ISABE-2009-1293.

[20] Paradiso, B., Persico, G., Gaetani, P., Schennach, O., and Woisetschläger, J., 2008. "Blade row interaction in a one and a half stage transonic turbine focusing on three dimensional effects: part 1 - stator-rotor interaction". In Proceedings of ASME Turbo Expo 2008, June 9-13, Berlin, Germany, ASME Paper GT2008-50291.